European **J**ournal of **Chem**istry

Characterization of PLA nanofiber structures containing herbal extracts

Nilsen Sunter Eroglu [ID] 1,* and Suat Canoglu [ID] 2

1 Department of Textile and Fashion Design, Faculty of Fine Arts, Halic University, Istanbul, 34421, Turkey
2 Department of Textile Engineering, Faculty of Technology, Marmara University, Istanbul, 34730, Turkey

* Corresponding author at: Department of Textile and Fashion Design, Faculty of Fine Arts, Halic University, Istanbul, 34421, Turkey.
 e-mail: nilseneroglu@halic.edu.tr (N.S. Eroglu).

RESEARCH ARTICLE

ABSTRACT

The use of renewable, sustainable, and biocompatible products without chemical side effects is increasing day by day in antibacterial applications instead of materials that harm nature and humans. In biomedicine, antibacterial nanofiber composite surfaces with generally produced from materials with antibacterial properties such as chitosan, hyaluronic acid, collagen, and silver nanoparticles. In this study, olive leaf, terebinth, and fumitory plants and biocompatible, biodegradable, and environmentally friendly polylactic acid (PLA) polymer were used to obtain nanofiber structures with 100% plant extracts. Viscosity and conductivity of solutions prepared with optimum properties were analysed, the nanofiber material was produced in solution with electrospinning method, and the morphological evaluation and mechanical measurement of the nanofiber material were performed. Finally, bacterial exchange analyses were performed before and after incubation in the UV-VIS spectrophotometer. As a result of the study, the thinnest and the most uniform fiber materials were found in CFO (consist of PLA (C1) and fumitory (FO)) coded nanofiber material, the best strength values were found in COE (consist of PLA (C1) and olive leaf (OE)) coded nanofiber structure, and the highest bacterial exchange was observed in CFO coded nanofiber material. Based on these results, it has been suggested that the CFO coded nanofiber structure can be used in biomedicine. It has been observed that olive leaf, terebinth, and fumitory plant extracts, which can be grown easily in every region in Turkey, have a significant level of bacterial resistance. In conclusion, fumitory and terebinth plants can be used in antibacterial agent applications since they allow obtaining smooth and uniform nanofiber structures, and thanks to their high bacteria nullification properties.

Journal website: www.eurjchem.com

1. Introduction

In nature, animals, humans, and plants are in an ecological balance. Plants are the source of nutrients for all living things. According to archaeological findings, humans have been using plants for nutrition and health since ancient times. Plants can transform water, minerals, and some other substances (essential oils, alkaloids, tannins, *etc.*) they take from the soil in their metabolism and turn them into other compounds (carbohydrates, water, proteins, fats, vitamins, and minerals) that people can digest. This strengthens the defence mechanism of the human body, supports the function of organs, and facilitates the healing of scar tissues. The importance and industrial use of medicinal and aromatic plants have increased with the development of modern medical science. In Turkey, 347 different plant species grow in nature and are traded, and nearly 30% of them are exported [1]. Plants have some beneficial properties such as antibacterial, anti-inflammatory, antiviral, antitumor, antioxidant, and anticancer activity. It is thought that the use of various therapeutic plants will increase in several fields in medical science. Nanofiber production through electrospinning has attracted attention for its applications in many fields such as tissue engineering, drug release, filtration, food industry, cosmetics, agriculture, and bio-

detection. Although synthetic-based polymer materials are generally used in these applications, approaches of using biocompatible, biodegradable, and toxic-free natural agents with few side effects are becoming more popular [2-5].

Polylactic acid (PLA) used in this study is the most popular polymer in the medical applications due to its biostructure and biocompatible and biodegradable properties [6]. It is a thermo-plastic polymer, structurally from the a-hydroxy acid family. PLA is obtained as a product of starch fermentation of plants such as corn, sugar cane, potatoes, and beets. In general, PLA has high mechanical strength and modulus, but low impact strength, low temperature of use, and relatively low machin-ability [7]. PLA has various molar masses, microstructures, and crystallinity and is used in the preparation of drug carriers and temporary medical implants [6]. Otherwise, absorbable sutures are used in many biomedical applications, including stents and orthopaedic plates and screws, anti-adhesive films, drug tissue engineering scaffolds, and absorbable implantable devices and coatings [8]. PLA was chosen for this research because of its promising biological properties in the field of biomedicine.

The first plant used in this study is the olive leaf. Mostly produce in the Mediterranean region, the olive (Olea *europaea*) has attracted more attention in recent years due to its positive effects on human health.
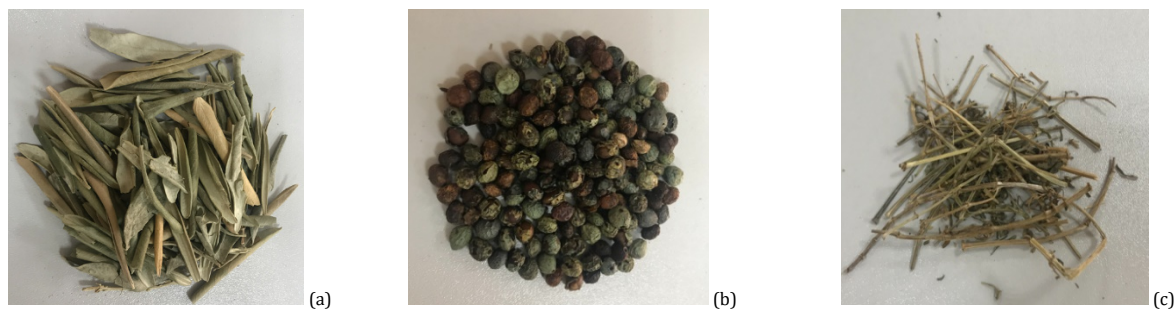
Figure 1. Olive leaf, terebinth, and fumitory samples.

In the Mediterranean diet, the nutritional model of olive oil is known to decreased rates of risks coronary heart disease risks [9]. The fact that olive, which is the most important element of the Mediterranean diet, has phenolic compounds are highly bioavailable [10], has spread its use as an active agent. Many researchers [11-17] have observed the ability of oleuropein, which is abundant in the olive leaf, to delay and inhibit the growth rate of microorganisms. Researchers report that apart from oleuropein, hydroxytyrosol, 4-hydroxybenzoic acid, vanillic acid, and *p*-coumaric acid components also have antibacterial effects. The antibacterial effect of olive leaf has been proven by many studies. Electrospun structures formed by olive leaf extract showed strong resistance against *E. coli*, *P. aeruginosa* and *B. subtilis* bacteria [18]. It is possible to increase the efficiency of *E. coli*, *S. aureus* and *C. albicans* bacteria by changing the extract ratio of olive leaf [12]. Similarly, in another study, antibacterial capacity was observed in the form of *B. cereus ~ C. albicans > E. coli > S. aureus > C. neoformans ~ K. pneumoniae ~ P. aeruginosa > B. subtilis* with the change of extract concentration. It has been stated that this difference in the effect of oleurepein on bacteria is due to the difference in the cell structure of each bacterium [14].

Different parts of terebinth, which is the second type of plant used in this study, are used as an aphrodisiac, anti-inflammatory, antiseptic, and antihypertensive, and in the treatment of dental and gastrointestinal diseases, wounds and burns, rheumatism, liver, urinary tract, and respiratory tract diseases [19-20]. Terebinth is the most common plant species of the family because it is resistant to cold and drought, and it turns into pistachio with grafting [21]. Many researchers have observed that terebinth fruit has antioxidant, antimicrobial, antiviral, anticholinesterase, anti-inflammatory, antinociceptive, antidiabetic, antitumor, antihyperlipidemic, antiatherosclerotic, and hepatoprotective effects [19,22-23]. It has been observed that the nanofiber structures formed by the polyvinyl alcohol (PVA) and polycaprolactone (PCL) polymers of the Trenbinth plant show resistance against bacteria in the order of *C. albicans > E. coli > P. aeruginosa > B. subtilis* [18].

The third and last plant species used in this examination, fumitory (*Fumaria officinalis*), is in the *Fumariaceae* sub-family of the *Papaveraceae* family. Fumaria officinalis contains some chemical constituents like alkaloids, carbohydrates, phenolic compounds, flavonoids, glycosides, terpenoids, phytosterols, proteins, amino acids, saponins, fixed oils, steroids, tannins. The plant is contained alkaloids isoquinoline-type [24]. It has therapeutic properties against stomach and digestive tract disorders thanks to this alkaloid content [25]. Bactericidal activities against the Gram-positive organisms of Fumaria officinalis have been known [24]. In the studies of Dülger and Gönüz, it was determined that the extract of fumitory was active against *E. coli*, *S. aureus*, *K. pneumoniae*, *P. aeruginosa*, *P. vulgaris*, *B. cereus*, *M. luteus*, *M. smegmatis*, *C. albicans*, *K. fragilis*, and *R. rubra* bacteria [26].

In the literature, there are several researches on obtaining nanofiber materials by mixing different herbal extracts with polymer materials and using them in the medical field. For example, olive leaves have a high potential for tissue scaffolding in biomedical applications thanks to its high antioxidant effect [12] Electrospun mats with olive leaf therapeutic agents to infected skin wounds [27], coaxial nanofiber design by using olive leaf extract as a bioactive agent [28]. It is known that fumitory and trenbinth plants form electrospun structure with PVA and PCL and show bacterial resistance [18]. However, there is still a need for some research on multifunctional membranes that enable antipathogen activities, drug delivery systems with time-controlled release, and sterilized food packaging materials and the materials to be used for these researches. Based on this thought, within the scope of the case, olive leaves and lesser-known fumitory and terebinth plants, which can be grown easily in Turkey due to the climate, have been used. The most significant issue that emerged in these studies is the macromolecule compatibility between the herbal extract and the polymer material and the formation of a smooth surface. The rate of plant material used in this experimental study was determined as 15%. The cause for this is the ability to observe the bacterial exchange effect by using the highest possible plant ratio. Herbal extracts were obtained with the Soxhlet extraction method and mixed with PLA until they became a homogeneous solution. Then, the nanofiber material was produced by using the electrospinning method in the prepared solutions, and characterization, mechanical, and bacterial change tests were performed on these structures. By analysing these measurements, the optimum level of herbal extract/polymer substance was determined. The nanofiber material suitable for use in the biomedical field has been proposed after examining the values obtained.

2. Experimental

2.1. Materials

PLA polymer was used by making it homogeneous. PLA $((C_3H_4O_2)_n)$ in 2003D coded bead structure was obtained from NatureWorks LLC (Minnetonka, USA), MN. In addition, dimethyl formamide (Merck), ethanol (Merck), methanol (Merck), chloroform (Merck), acetone (Merck) and distilled water are used to dissolve polymer and herbal extracts used. Herbal extraction was prepared with olive leaf plant (Figure 1a) in leaf form, terebinth plant (Figure 1b) in seed form, and fumitory plant (Figure 1c) in leaf and stem form. All herbs used were packaged within the last 3 months (2020) and purchased from a local brand, Aktar Diyarı (Izmir, Turkey).

2.2. Preparation of herbal extracts

Plant parts were washed two times with distilled water to avoid dust and similar residues and dried in an oven at 70 °C for 10 minutes.

Table 1. Preparation of herbal extraction.

Herbal extract	Concentration of extracted part (%wt)	Solvent type (v/v)	Temperature of mixing (°C)	Stir of mixing (rpm)	Time of mixing (h)	Reference
Olive leaf	25	Methanol/Water (4:1)	Room	300	24	[30]
Fumaria officinalis	10	Methanol	Room	300	4	[31]
Pistacia terebinthus	30	Ethanol	Room	300	6	[21]

Table 2. Experimental design for electrospinning process *.

Polymer structure	Herbal extract	Feeding rate (mL/h)	Applied voltage (kV)	Distance between syringe needle and collector (cm)	Temperature of process (°C)	Time of production (h)
C1	-	1.6	28	20	22	3
CFO	Fumaria officinalis (FO)	1.6	29	20	26	3
CPT	Pistacia terebinthus (PT)	1.6	29	20	24	3
COE	Olive leaf (OE)	1.6	32	20	20	3

* PLA Polymer Code: C.

Soxhlet extraction could extract more herbal sample mass than the latest alternatives and subject to no matrix effects. For this reason, it was preferred in this study. Extraction was repeated for each plant species with the Soxhlet extraction method, which is a method of extracting essential oil from plants [29]. To prevent the loss of solvent by evaporation, a condenser was used. The herbal extracts were filtered using 2 pieces of filter paper and the solvent was removed using an evaporator at 38 °C at 120 rpm rotation. Herbal extraction preparation parameters are given in Table 1.

2.3. Preparation of solutions for electrospinning

In the study, firstly, the polymer solution was ensured that 8% (percentage wt.) PLA was dissolved at room temperature in three hours at a ratio of dimethylformamide:chloroform (1:9, v:v) at 600 rpm until it became homogeneous. Homogeneous mixing and concentration of the herbal extract/polymer material are two essential factors to reveal the activity of the antibacterial components in the herbal extract. As a result of the tests conducted, the herbal substance ratio was determined as 15%, since the concentration of the herbal extract in the polymer had more efficient results in terms of determining the fiber morphology and chemical properties. The prepared mixture was stirred in a magnetic stirrer for 45 minutes to ensure homogeneity.

2.4. Viscosity and conductivity measurement parameters of polymer/herbal extract solutions

2.4.1. The viscosity measurement of polymer/herbal extract solutions

The viscosities of polymer solutions were measured using a viscometer device (Brookfield DV-E Viscometer, USA). Viscosity measurement was made using S21 spindle type at 100 rpm. The viscosity values of all prepared solutions according to the shear rate are expressed in cP (centipoise). Two replicate tests were performed for each measurement.

2.4.2. The conductivity of polymer/herbal extract solutions

The conductivity values of polymer solutions were measured with a portable electrical conductivity meter (WTW Cond 3110, Germany). The conductivity measurement probe was immersed in the prepared solution and measured in mS/cm. Viscosity and conductivity measurements were made under laboratory conditions (23±2 °C and 45±10 % RH).

2.5. Production of PLA based electrospun fibers

In the study, after the solution was prepared and the characterization measurements were made, 8 mL of solution was taken with a 10 mL syringe. Then, nanofiber structure production was achieved by providing the values specified in

Table 2 at a rotation speed of 100 rpm on oil paper with a syringe placed in the Inovenso NE 300 Nano Spinner brand electrospinning device.

2.6. Morphology and structure characterization of herbal extracts-based nanofiber structures

The morphologies of the herbal-based nanofibers produced in the study were investigated with JEOL JSM-IT100 Scanning Electron Microscopes (SEM). The morphologies of herbal-based nanofiber structures were analysed using SEM device at 1000- and 20000-times magnification. Image J software was used to measure the fiber diameters of the images with 15 repetitions, and SPSS 24 statistical program was used to obtain the diameter distribution charts. Nicolet is10, Thermo Scientific brand device was used in the Fourier Transformed Infrared Spectrum (FTIR) examination of the obtained nanofiber structures. For both measurements, samples of 10×10 mm were taken.

2.7. Mechanical tests of herbal extract-based nanofiber structures

Thickness, tensile strength, and elongation at break measurements were made to measure the effect of vegetable matter on strength in herbal-based nanofiber structures produced in the study. Thickness measurements were made with Mitutoyo Digital Thickness Comparator (Mitutoyo, Kawasaki, Japan) device in "mm" from 10 different points in vertical and horizontal directions. These values were used to measure strength measurements in megapascals (MPa). Tensile strength and elongation at break values of samples taken from 50×10 mm (length×width) dimensions were measured in Instron 4411 Universal tester (Instron, Norwood, MA, USA).

2.8. UV-VIS bacteria change measurements

In the bacterial change measurement, dilutions were made in the broth (mL) which decreased by two times [32] (Table 3). A standard final concentration of the dilution was prepared, and the herbal extracts were added in equal proportions (1 mL) to each tube containing various dilutions [32]. Bacterial growths were observed by absorbance measurements before and after the incubation process.

In the study, the first operation was bacterial cultivation. For this step, the liquid medium was prepared by using 250 mL of distilled water and 2 g (Nutrient broth). 50 mL of medium was taken from the bottle, some bacteria were scraped from the petri dish with a sterile disposable stick, and the bacteria were cultivated into falcon tubes and it is incubated.

For reference measurement, 0.1 g Nutrient Broth medium was prepared with 12.5 mL distilled water, solutions containing reference mixture in the st cuvette, *P. aeruginosa* (PA) in the 2nd cuvette, *B. subtilis* (BS) in the 3rd cuvette, *S. aureus* (SA) in the 4th cuvette, *E. coli* (EC) bacteria in the 5th cuvette were placed in

Table 3. Bacteria measurement values.

Ingredients	Medium (1st cuvette)	*P. aeruginosa* (2nd cuvette)	*B. subtilis* (3rd cuvette)	*S. aureus* (4th cuvette)	*E. coli* (5th cuvette)
1 mL medium + bacteria	0	0.090	0.066	0.267	0.231
1 mL medium + bacteria + pure water	0	0.756	0.125	0.442	0.460

Table 4. Mixing ratio of tubes.

Tube	Polymer structure liquid (mL)	Isotonic NaCl (mL)	Bacteria (mL)
1	1	4.0000	5.0000
2	1	6.5000	2.5000
3	1	7.7500	1.2500
4	1	8.3750	0.6250
5	1	8.6875	0.3125
6	1	8.8432	0.1568
7	1	8.9220	0.0780
8	1	8.9610	0.0390

Table 5. The viscosity and conductivity of C group solutions.

Polymer samples	Viscosity (cP)	Torque rating (%)	Conductivity (µS/cm)	Temperature (°C)
C1	155	31.1	0.2	22
CFO	81.5	16.3	35.9	26
CPT	71.5	14.3	1.6	24
COE	170	34.0	18	20

a UV-VIS spectrophotometer and measurements were performed at 600 nm. Tubes without herbal extract but containing microorganisms and medium (1st cuvette) were used as a positive control. The presence of bacteria was confirmed by comparing the values seen in other cuvettes (Table 3).

For the preparation process in the study, the first 4.5 g isotonic NaCl to be used in the bacteria mixture, and 500 mL distilled water mixture was prepared. In order to obtain the polymer structure liquid, autoclaved isotonic NaCl solution 100 times the polymer structure weight was transferred to the Falcon tube and the prepared polymer liquid solution was incubated at a shaking incubator. Then, the water of the polymer structure, isotonic NaCl, and bacteria were added to 8 Mc Farland tubes for each bacterium, and the mixture was prepared at the rates indicated in the table. In this process, the aim was to mix the antibacterial effect of the nanofiber structures into the solution, and dilution was applied for each tube, and bacteria were added at different concentrations (Table 4). In the investigation, bacteria measurements of the prepared mixtures were performed. UV-VIS spectrophotometer measurements were performed, and it was observed how the antibacterial factors in the nanofiber structures affected the bacteria with the change of time.

3. Results and discussion

3.1. Results of viscosity and conductivity measurement parameters of solutions

The resistance of a solution to flow under surface tension determines its viscosity. Viscosity is the most important parameter that determines the flow rate of the solution. Viscosity is related to the degree of entanglement of polymer molecule chains in solution. Beaded fibers are more likely to be obtained rather than straight fibers at low viscosity, where there is usually a polymer chain. In general, since the polymer chain is more difficult to synthesize with each other [33], less chain entanglement occurs, and jet stability is lost. As a result, the fibers are collected into the collector as droplets, and the droplets first turn into spindle-like structures and then into beaded nanofibers [12]. Therefore, the factors affecting the viscosity of the solution also affect the electrospinning process and the resulting fibers [34]. As a result of the study, the viscosity values of the nanofiber structure groups are listed as COE > C1 < CFO > CPT (Table 5). When the results were

examined, it was seen that the COE group fibers formed more regular and uncomplicated structures.

The low conductivity value leads to the formation of beaded nanofiber structures with larger sizes [35]. Correspondingly, more regular and finer nanofibers are formed as the conductivity of polymer solution increases [36]. It is known that this situation results from the increase in the attraction of the polymer jet in the electric field with the increase in charge density [37]. In the conductivity tests, it was observed that the highest values belonged to the CFO (255.6 nm) group nanofiber structures. The fact that CFO group nanofiber structures have the most uniform, smooth, and beadless structures and have lower fiber diameters from the four nanofiber structure groups supports this idea (C1 (359.73 nm), COE (441.87 nm), and CPT (513.87 nm).

3.2. Determination of morphology and structure characterization of herbal extract-based nanofiber structures

3.2.1. Surface characterization of herbal extract-based nanofiber structures

In the study, the fiber diameter fineness (nm) of group C nanofiber structures is listed as CPT > COE > C1 > CFO (Figures 2 and 3). The smooth and uniform structure, which has the thinnest fibers among the C group nanofiber structures, was observed in the CFO nanofiber structure. It was observed that fumitory plant and PLA polymer provided good morphological compatibility and fine, smooth, uniform nanofiber formation was obtained. It is known that the fumitory plant, which has limited literature, is used in many treatment methods with its high alkaloid content (60-70%) [38]. It is thought that the nanofiber structure containing fumitory will also have good properties in terms of fineness and antibacterial properties. Since there are two different components in plant-based nanofiber structures, nanofiber surfaces were formed in more branched structures compared to the pure polymer C1 sample without plant content. This situation is clearly observed in the SEM images.

3.2.2. FTIR characterization of herbal extract-based nanofiber structures

FTIR analysis was used in order to define the internal bonds of the molecular structures of the obtained nanofibers.
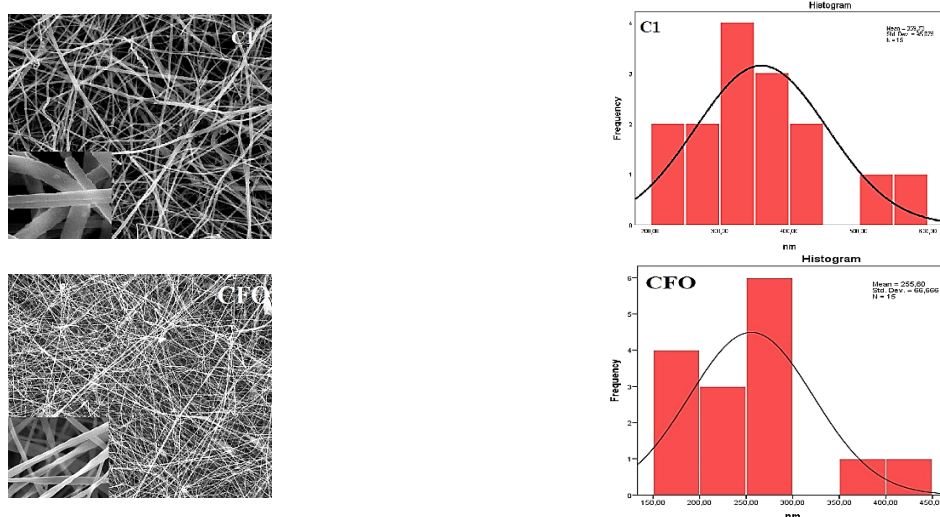
Figure 2. SEM images (1000 and 20,000×) and distribution of diameter (20,000×) of C1 and CFO nanofiber structures.
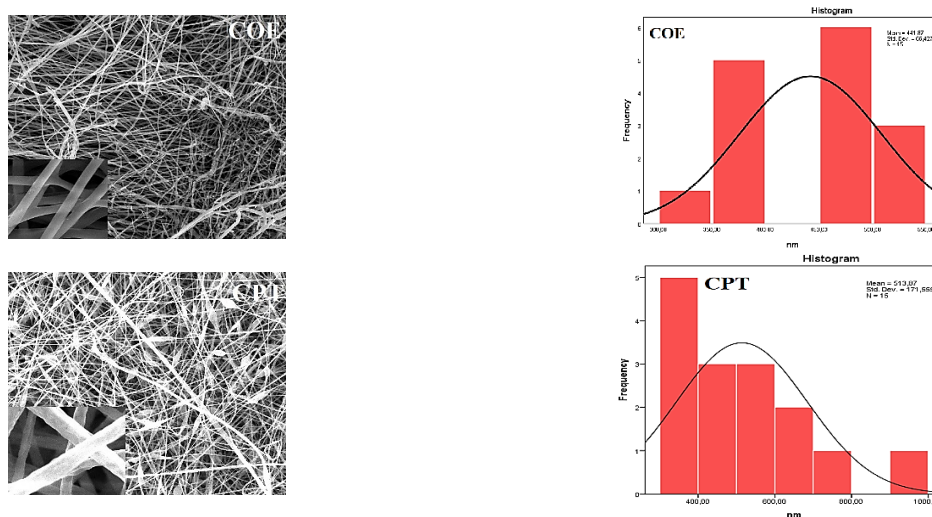
Figure 3. SEM images (1000 and 20,000×) and distribution of diameter (20,000×) of COE and CPT nanofiber structures.

The method is based on the absorption of infrared rays falling on the bonds with vibration and rotational motion in correlation. In the infrared spectra obtained, the presence and effectiveness of herbal extracts and polymer material were analyzed.

In all FTIR spectra of the surfaces obtained as a result of the study, the wavelength is in the range of 450-4000 cm^{-1} for all C group samples. In the analyses, the effects of characteristic bands in herbal extracts on the obtained nanofiber structures were investigated. Therefore, comparative analyses were carried out with the pure polymer (C1) that did not contain the extract. According to this, =C-H bonds are seen in C1 polymer at absorbance values of 754 and 867 cm^{-1}, C–O bond related to −CH(C H3) −OH at 1084 and 1181 cm^{-1}, asymmetrical C–H bond at 1359 cm^{-1}, symmetrical −CH$_3$ bond at 1451 cm^{-1}, carbonyl C=O bond at 1750 cm^{-1}, and vibration of C-H bonds at 2995 and 3005 cm^{-1} [39].

The cause for the 1022 cm^{-1} peak of the FO extract in the FTIR spectrum with the fumitory plant content is due to the presence of =C-H bonds [40]. The fact that the wavelength of the CFO polymer is different at 1005 cm^{-1} compared to the C1 polymer is interpreted as the effect of the fumitory extract.

In the FTIR spectrum of the terebinth plant, a broad absorption peak was observed at approximately 3327 cm^{-1},

corresponding to the −OH stretch. Polyphenolic structures have an absorption peak with C–H symmetric stretching vibrations around 2974 cm^{-1}. C=O stretching vibrations are observed at 1655 cm^{-1}. The peaks around 1380 cm^{-1} are formed by the contribution of aromatic C=C bonds. Out-of-plane C–H bending vibrations of the aromatic ring were observed in the range of 623-879 cm^{-1} [41]. The peak at a wavelength of 1045 cm^{-1} in terebinth extract indicates the stretching of C-N bonds [42]. This peak affected on group C nanofibers. The presence of PT extract is seen at 1023 cm^{-1} in CPT nanofiber structures.

Olive leaf contains main ingredients such as oleuropein and hydroxytyrosol. The primary components of the compound can be determined from the structures of the phenol O-H, carboxylic acid C=O, and alkene C=C stretch nodes observed at 3307 cm^{-1}. In addition, the 1651 cm^{-1} peak corresponds to the presence of amide I [43]. It indicates the CH stretches of the characteristic bands at 2835-2946 cm^{-1} peaks, the C-O stretching of phenols in the 1111-1411 cm^{-1} absorption region, and the presence of aromatic rings of olive leaf polyphenols at 1449 cm^{-1} [39]. Conclusively, the peak observed at 1017 cm^{-1} is considered to be indicative of the CN stretching vibration of the amine group [43]. The subsistence of olive leaf extract is seen at 1015 cm^{-1} in the COE nanofiber structure.
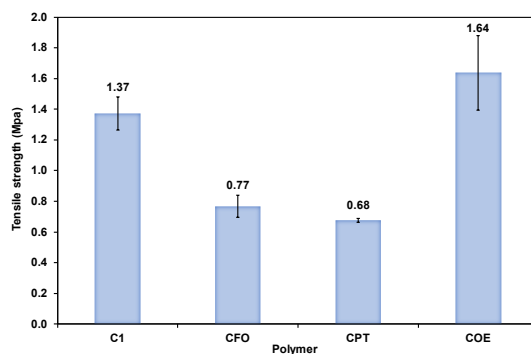
Figure 4. Tensile strength in the machine direction of C groups nanofiber structures.
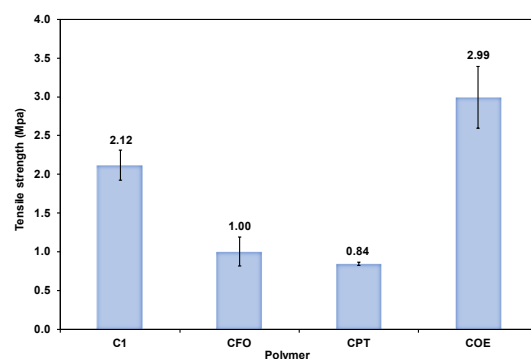
Figure 5. Tensile Strength in the material width direction of C groups nanofiber structures.
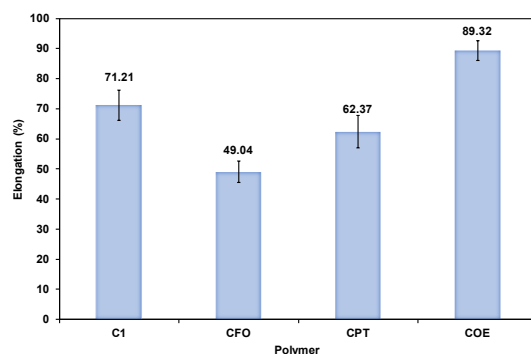
Figure 6. Elongation in the machine direction of C group nanofiber structures (%).

3.3. Mechanical tests result of herbal extracts-based nanofiber structures

3.3.1. Tensile Strength Results of herbal extracts-based nanofiber structures

The strength of a material increases as the length of its polymer chain and the number of cross-links between its polymer chain increase [37]. At this stage of the study, it was aimed to measure and evaluate the effects of plant materials on strength in nanofiber constructions. In this sense, vertical (machine direction) and horizontal (material width) breaking strength values were restrained and analyzed.

The order of machine direction and material width strength averages of C group nanofiber structures was COE > C1> CFO > CPT (Figures 4 and 5). When the sequence was examined, it was observed that the CFO and CPT nanofibers decreased the breaking strength compared to the C1 nanofiber. PLA, the main material of group C nanofibers, is a polymer with high biodegradability, biocompatibility, thermoplastic process-ability, and mechanical properties [44]. When the chemical crosslink structure is defined in PLA, the material first hardens compared to pure PLA, but then it becomes more brittle over time and there is a sudden decrease in strength. After PLA hardens, it becomes brittle with increasing bond density [45]. It is thought that this structural change of PLA may have reduced the nanofiber strength by making the nanofiber formation brittle, depending on the addition of herbal extracts in CFO and CPT nanofibers and the binding status of the extract. In the COE nanofiber structure, an increase in strength is observed with the hardening of the PLA polymer.

3.3.2. Elongation at break tests of herbal extract-based nanofiber structures

Elongation at break tests was performed in two different positions, similar to the tensile strength tests, by considering the machine direction (vertical) and the material width direction (horizontal) (Figures 6 and 7).

Table 6. UV-VIS bacterial exchange measurements of *P. aeruginosa* and *B. subtilis* bacteria for COE nanofiber structures.

First measurement				Second measurement			
PA codes	Absorbance	BS codes	Absorbance	PA codes	Absorbance	BS codes	Absorbance
OE-PA-1	0.043	OE-BS-1	0.038	OE-PA-1	0.042	OE-BS-1	0.041
OE-PA-2	0.024	OE-BS-2	0.019	OE-PA-2	0.027	OE-BS-2	0.016
OE-PA-3	0.008	OE-BS-3	0.009	OE-PA-3	0.012	OE-BS-3	0.033
OE-PA-4	0.003	OE-BS-4	0.003	OE-PA-4	0.005	OE-BS-4	0.006
OE-PA-5	0.002	OE-BS-5	0.001	OE-PA-5	0.000	OE-BS-5	0.000
OE-PA-6	0.000	OE-BS-6	0.001	OE-PA-6	0.000	OE-BS-6	0.000
OE-PA-7	0.001	OE-BS-7	0.000	OE-PA-7	0.000	OE-BS-7	0.001
OE-PA-8	0.001	OE-BS-8	0.000	OE-PA-8	0.000	OE-BS-8	0.000
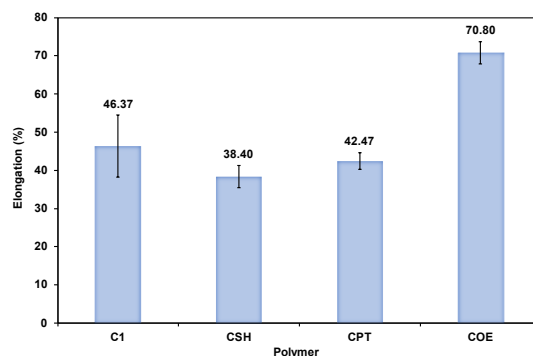
Figure 7. Elongation in the material width direction of C group nanofiber structures (%).
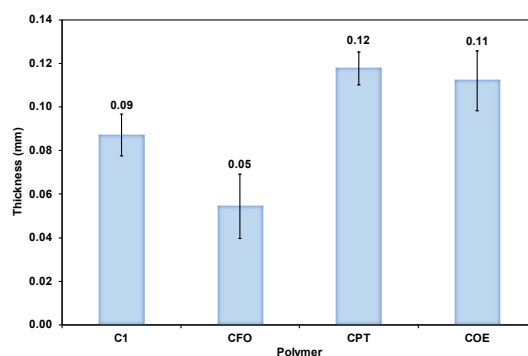
Figure 8. Nanofiber structures thicknesses of group C.

In the measurements performed, it was observed that there was no direct relationship between the herbal extract addition and the flexibility of the nanofiber structures.

3.3.3. Thickness of herbal extract-based nanofiber structures

The thicknesses of the obtained nanofibers in the horizontal and vertical directions were measured in mm. In the fiber fineness distributions of the SEM measurements made within the scope of the study, it was observed that the CFO nanofiber structure consisted of thinner fibers than other nanofiber structures. This situation is associated with the combination of fiber groups consisting of fine fibers and forming a surface in a thinner layer.

In the results examined, it was not possible to make a clear inference about the effect of herbal extracts on the nanofiber structure thickness. While the addition of herbal extract in the CFO nanofiber structure increased the structure thickness, it decreased the structure thickness in CPT and CFO structures. This is related to the morphological compatibility between the polymer and the herbal extract and does not form a link between the plant ingredients (Figure 8).

3.4. UV-VIS bacteria change results of herbal extract-based nanofiber structures

In the study, UV-VIS spectrophotometer measurements of the mixtures of COE, CPT, and CFO nanofiber samples were performed before and after the incubation process. Shaking in the incubator was performed for 1 hour at 37 °C. It was recognized how much bacteria were affected over time. Eight replicates and two parallel absorbance measurements were made for each bacterium. The absorbance values were measured at 600 nm before and after incubation with *P. aeruginosa*, *B. subtilis*, *S. aureus*, and *E. coli* bacteria used in the study and the values given in Tables 6-11 were obtained. The first measurement indicated in the tables refers to the pre-incubation, the second measurement refers to the post-incubation.

As seen in Table 4, a decrease was observed in the number of bacteria prepared at disparate concentrations. In the first and second measurements before and after incubation, absorbance measurements deteriorated as the bacterial concentration decreased. When the bacterial optical density (OD) values obtained from the UV-VIS spectrophotometer of COE, CPT, and CFO nanofibers are examined, it is seen that they are listed as CFO > CPT > COE.

Table 7. UV-VIS bacterial exchange measurements of *S. aureus* and *E. coli* bacteria for COE nanofiber structures.

First measurement				Second measurement			
SA codes	Absorbance	EC codes	Absorbance	SA codes	Absorbance	EC codes	Absorbance
OE-SA-1	0.168	OE-EC-1	0.121	OE-SA-1	0.163	OE-EC-1	0.144
OE-SA-2	0.078	OE-EC-2	0.070	OE-SA-2	0.074	OE-EC-2	0.071
OE-SA-3	0.049	OE-EC-3	0.035	OE-SA-3	0.032	OE-EC-3	0.033
OE-SA-4	0.011	OE-EC-4	0.021	OE-SA-4	0.009	OE-EC-4	0.015
OE-SA-5	0.008	OE-EC-5	0.007	OE-SA-5	0.010	OE-EC-5	0.006
OE-SA-6	0.009	OE-EC-6	0.016	OE-SA-6	0.004	OE-EC-6	0.004
OE-SA-7	0.001	OE-EC-7	0.005	OE-SA-7	0.010	OE-EC-7	0.003
OE-SA-8	0.000	OE-EC-8	0.003	OE-SA-8	0.000	OE-EC-8	0.000

Table 8. UV-VIS bacterial exchange measurements of *P. aeruginosa* and *B. subtilis* bacteria for CPT nanofiber structures.

First measurement				Second measurement			
PA codes	Absorbance	BS codes	Absorbance	PA codes	Absorbance	BS codes	Absorbance
PT-PA-1	0.101	PT-BS-1	0.024	PT-PA-1	0.112	PT-BS-1	0.031
PT-PA-2	0.058	PT-BS-2	0.015	PT-PA-2	0.059	PT-BS-2	0.041
PT-PA-3	0.027	PT-BS-3	0.006	PT-PA-3	0.047	PT-BS-3	0.015
PT-PA-4	0.015	PT-BS-4	0.000	PT-PA-4	0.009	PT-BS-4	0.007
PT-PA-5	0.008	PT-BS-5	0.002	PT-PA-5	0.007	PT-BS-5	0.001
PT-PA-6	0.005	PT-BS-6	0.001	PT-PA-6	0.003	PT-BS-6	0.001
PT-PA-7	0.001	PT-BS-7	0.000	PT-PA-7	0.000	PT-BS-7	0.001
PT-PA-8	0.001	PT-BS-8	0.000	PT-PA-8	0.000	PT-BS-8	0.003

Table 9. UV-VIS bacterial exchange measurements of *S. aureus* and *E. coli* bacteria for CPT nanofiber structures.

First measurement				Second measurement			
SA codes	Absorbance	EC codes	Absorbance	SA codes	Absorbance	EC codes	Absorbance
PT-SA-1	0.030	PT-EC-1	0.133	PT-SA-1	0.045	PT-EC-1	0.132
PT-SA-2	0.015	PT-EC-2	0.080	PT-SA-2	0.042	PT-EC-2	0.093
PT-SA-3	0.012	PT-EC-3	0.045	PT-SA-3	0.036	PT-EC-3	0.055
PT-SA-4	0.013	PT-EC-4	0.025	PT-SA-4	0.015	PT-EC-4	0.027
PT-SA-5	0.017	PT-EC-5	0.015	PT-SA-5	0.011	PT-EC-5	0.018
PT-SA-6	0.011	PT-EC-6	0.037	PT-SA-6	0.005	PT-EC-6	0.015
PT-SA-7	0.001	PT-EC-7	0.001	PT-SA-7	0.002	PT-EC-7	0.006
PT-SA-8	0.000	PT-EC-8	0.002	PT-SA-8	0.004	PT-EC-8	0.007

Table 10. UV-VIS bacterial exchange measurements of *P. aeruginosa* and *B. subtilis* bacteria for CFO nanofiber structures.

First measurement				Second measurement			
PA codes	Absorbance	BS codes	Absorbance	PA codes	Absorbance	BS codes	Absorbance
FO-PA-1	0.229	FO-BS-1	0.078	FO-PA-1	0.250	FO-BS-1	0.078
FO-PA-2	0.144	FO-BS-2	0.055	FO-PA-2	0.154	FO-BS-2	0.055
FO-PA-3	0.170	FO-BS-3	0.038	FO-PA-3	0.168	FO-BS-3	0.038
FO-PA-4	0.075	FO-BS-4	0.021	FO-PA-4	0.081	FO-BS-4	0.021
FO-PA-5	0.056	FO-BS-5	0.016	FO-PA-5	0.051	FO-BS-5	0.016
FO-PA-6	0.042	FO-BS-6	0.013	FO-PA-6	0.038	FO-BS-6	0.013
FO-PA-7	0.011	FO-BS-7	0.005	FO-PA-7	0.011	FO-BS-7	0.005
FO-PA-8	0.007	FO-BS-8	0.001	FO-PA-8	0.007	FO-BS-8	0.001

Table 11. UV-VIS bacterial exchange measurements of *S. aureus* and *E. coli* bacteria for CFO nanofiber structures.

First measurement				Second measurement			
SA codes	Absorbance	EC codes	Absorbance	SA codes	Absorbance	EC codes	Absorbance
FO-SA-1	0.216	FO-EC-1	0.232	FO-SA-1	0.216	FO-EC-1	0.234
FO-SA-2	0.138	FO-EC-2	0.144	FO-SA-2	0.180	FO-EC-2	0.148
FO-SA-3	0.075	FO-EC-3	0.110	FO-SA-3	0.105	FO-EC-3	0.102
FO-SA-4	0.014	FO-EC-4	0.077	FO-SA-4	0.074	FO-EC-4	0.067
FO-SA-5	0.000	FO-EC-5	0.030	FO-SA-5	0.078	FO-EC-5	0.051
FO-SA-6	0.006	FO-EC-6	0.020	FO-SA-6	0.064	FO-EC-6	0.036
FO-SA-7	0.015	FO-EC-7	0.015	FO-SA-7	0.009	FO-EC-7	0.019
FO-SA-8	0.008	FO-EC-8	0.006	FO-SA-8	0.008	FO-EC-8	0.008

This means that the antibacterial inhibitory effect of the CFO nanofiber was higher, and it nullified the number of bacteria at a higher rate. Absorbance measurements for COE and CFO nanofibers were reset after eight replicate assessments. Even though the absorbance value for the CPT nanofiber decreased, it was not reset. Hereby, the lowest absorbance value without any visible turbidity, which prevents the growth of bacteria, was taken as the final value.

4. Conclusion

We tried to demonstrate nanofiber structures were obtained by incorporating olive leaf, fumitory, and terebinth herbal extract into PLA electrospun fibers by using the electrospinning method. The herbal extracts were included in the polymer solutions at a 15% rate and the conductivity and strength characterization measurements of the solutions were performed. Characterization measurement results determined the structural properties of nanofiber formations. The presence of herbal extracts in the nanofibers was confirmed by the appearance of the peaks in the FTIR analysis and the morphological appearances in the SEM images. In this study, it was observed that the thinnest fiber structures were CFO, the best strength values were COE, and the nanofiber structure with the highest bacterial exchange was CFO. In the bacterial exchange measurements, it was seen that the ability of the fumitory extract to nullify the number of bacteria was stronger than the extracts of olive leaf and terebinth. It has been concluded that the use of fumitory and terebinth plants, which are relatively less known than olive leaves and can easily grow in Turkey, as a source of strong environmentally friendly antibacterial substance has a great potential for future research. Further studies regarding the role of fumitory, and terebinth extracts in

nanofiber structures would be worthwhile. In this study, it was used that instead of chemical and synthetic antibacterial agents, which are known to be harmful to nature and human health, herbal extracts, and the PLA, which is mostly used in biomedical applications. Herbal extracts have the potential to be a resource for future biomedical research because they are environmentally friendly, biocompatible, sustainable, and economical. In addition, the production of herbal extracts by creating different ratios/ variations with different natural or chemical nanofiber structures in future research may allow for various purposes such as tissue engineering, wound dressing, drug release mechanisms in the medical field.

Acknowledgements

Disclosure statement ⒹⓈ

Conflict of interests: The authors declare that they have no conflict of interest.
Ethical approval: All ethical guidelines have been adhered.
Sample availability: Samples of the compounds are available from the author.

CRediT authorship contribution statement ⒸⓇ

Conceptualization: Nilsen Sunter Eroglu, Suat Canoglu; Methodology: Nilsen Sunter Eroglu, Suat Canoglu; Software: Nilsen Sunter Eroglu; Validation: Nilsen Sunter Eroglu, Suat Canoglu; Formal Analysis: Nilsen Sunter Eroglu; Investigation: Nilsen Sunter Eroglu; Resources: Nilsen Sunter Eroglu; Data Curation: Nilsen Sunter Eroglu, Suat Canoglu; Writing - Original Draft: Nilsen Sunter Eroglu, Suat Canoglu; Writing - Review and Editing: Nilsen Sunter Eroglu; Visualization: Nilsen Sunter Eroglu.

ORCID ⒾⒹ and Email ✉

Nilsen Sunter Eroglu
✉ nilseneroglu@halic.edu.tr
ⒾⒹ https://orcid.org/0000-0002-8403-7809
Suat Canoglu
✉ scanoglu@marmara.edu.tr
ⒾⒹ https://orcid.org/0000-0002-1604-9875

References

[1]. Göktaş, B.; Gidik, B. Bayburt ilinde doğadan toplanan tibbi ve aromatik bitkilerin tüketimi. *Res. Stud. Anatolia J.* **2019**, 303–311.

[2]. Yao, C.-H.; Yeh, J.-Y.; Chen, Y.-S.; Li, M.-H.; Huang, C.-H. Wound-healing effect of electrospun gelatin nanofibres containingCentella asiaticaextract in a rat model: Wound healing effect of EGC membrane. *J. Tissue Eng. Regen. Med.* **2017**, *11*, 905–915.

[3]. Karami, Z.; Rezaeian, I.; Zahedi, P.; Abdollahi, M. Preparation and performance evaluations of electrospun poly(ε-caprolactone), poly(lactic acid), and their hybrid (50/50) nanofibrous mats containing thymol as an herbal drug for effective wound healing. *J. Appl. Polym. Sci.* **2013**, *129*, 756–766.

[4]. Lin, S.; Chen, M.; Jiang, H.; Fan, L.; Sun, B.; Yu, F.; Yang, X.; Lou, X.; He, C.; Wang, H. Green electrospun grape seed extract-loaded silk fibroin nanofibrous mats with excellent cytocompatibility and antioxidant effect. *Colloids Surf. B Biointerfaces* **2016**, *139*, 156–163.

[5]. Motealleh, B.; Zahedi, P.; Rezaeian, I.; Moghimi, M.; Abdolghaffari, A. H.; Zarandi, M. A. Morphology, drug release, antibacterial, cell proliferation, and histology studies of chamomile-loaded wound dressing mats based on electrospun nanofibrous poly(ε-caprolactone)/polystyrene blends: Morphology, Drug Release, Antibacterial, Cell Proliferation, and Histology Studies. *J. Biomed. Mater. Res. B Appl. Biomater.* **2014**, *102*, 977–987.

[6]. Pretula, J.; Slomkowski, S.; Penczek, S. Polylactides—Methods of synthesis and characterization. *Adv. Drug Deliv. Rev.* **2016**, *107*, 3–16.

[7]. Saini, P.; Arora, M.; Kumar, M. N. V. R. Poly(lactic acid) blends in biomedical applications. *Adv. Drug Deliv. Rev.* **2016**, *107*, 47–59.

[8]. Langer, R.; Basu, A.; Domb, A. J. Special issue: Polylactide (PLA) based biopolymers. *Adv. Drug Deliv. Rev.* **2016**, *107*, 1–2.

[9]. Huang, C. L.; Sumpio, B. E. Olive oil, the mediterranean diet, and cardiovascular health. *J. Am. Coll. Surg.* **2008**, *207*, 407–416.

[10]. Omar, S. H. Oleuropein in olive and its pharmacological effects. *Sci. Pharm.* **2010**, *78*, 133–154.

[11]. Martín-Vertedor, D.; Garrido, M.; Pariente, J. A.; Espino, J.; Delgado-Adámez, J. Bioavailability of bioactive molecules from Olive leaf extracts and its functional value: Potential health benefits of Olive leaf extract. *Phytother. Res.* **2016**, *30*, 1172–1179.

[12]. Doğan, G. Elektrolif Çekim Yöntemiyle Elde Edilen Biyopolimer Nanoliflerin Doku Mühendisliği ve ilaç Salımı Uygulamalarında Kullanım Olanaklarının Araştırılması. Ph.D. Dissertation, Ege Üniversitesi, İzmir, Türkiye, 2012.

[13]. Fki, I.; Sayadi, S.; Mahmoudi, A.; Daoued, I.; Marrekchi, R.; Ghorbel, H. Comparative study on beneficial effects of hydroxytyrosol- and oleuropein-rich Olive leaf extracts on high-fat diet-induced lipid metabolism disturbance and liver injury in rats. *Biomed Res. Int.* **2020**, *2020*, 1315202.

[14]. Pereira, A. P.; Ferreira, I. C. F. R.; Marcelino, F.; Valentão, P.; Andrade, P. B.; Seabra, R.; Estevinho, L.; Bento, A.; Pereira, J. A. Phenolic compounds and antimicrobial activity of olive (Olea europaea L. Cv. Cobrançosa) leaves. *Molecules* **2007**, *12*, 1153–1162.

[15]. Sudjana, A. N.; D'Orazio, C.; Ryan, V.; Rasool, N.; Ng, J.; Islam, N.; Riley, T. V.; Hammer, K. A. Antimicrobial activity of commercial Olea europaea (olive) leaf extract. *Int. J. Antimicrob. Agents* **2009**, *33*, 461–463.

[16]. Markin, D.; Duek, L.; Berdicevsky, I. In vitro antimicrobial activity of olive leaves. Antimikrobielle Wirksamkeit von Olivenblattern in vitro. *Mycoses* **2003**, *46*, 132–136.

[17]. Balta, A. B. Development of natural compound loaded nanofibers by electrospinning, MSc Dissertation, İzmir Institute of Technology, The Graduate School of Engineering and Sciences, İzmir, Turkey, 2010.

[18]. Eroglu, S. N.; Canoglu, S.; Yuksek, M. Characterization, mechanical, and antibacterial properties of nanofibers derived from olive leaf, fumitory, and terebinth extracts. *Turk. J. Chem.* **2020**, *44*, 1043–1057.

[19]. Bozorgi, M.; Memariani, Z.; Mobli, M.; Salehi Surmaghi, M. H.; Shams-Ardekani, M. R.; Rahimi, R. Five Pistacia species (P. vera, P. atlantica, P. terebinthus, P. khinjuk, and P. lentiscus): a review of their traditional uses, phytochemistry, and pharmacology. *ScientificWorldJournal* **2013**, *2013*, 219815.

[20]. Topçu, G.; Ay, M.; Bilici, A.; Sarıkürkcü, C.; Öztürk, M.; Ulubelen, A. A new flavone from antioxidant extracts of Pistacia terebinthus. *Food Chem.* **2007**, *103*, 816–822.

[21]. Dogan, C. Menengiç ve Bazı Sert Kabuklu Meyve Dış Kabuklarına Ait Ekstraktların Antimikrobiyal ve Antioksidan Özelliklerinin Belirlenmesi ve Meyveli Yoğurt Üretiminde Kullanımı, Ph.D. Dissertation, Harran Üniversitesi, Şanlıurfa, Türkiye, 2016.

[22]. Giner-Larza, E. M.; Máñez, S.; Giner, R. M.; Recio, M. C.; Prieto, J. M.; Cerdá-Nicolás, M.; Ríos, J. L. Anti-inflammatory triterpenes from Pistacia terebinthus galls. *Planta Med.* **2002**, *68*, 311–315.

[23]. Benhammou, N.; Bekkara, F. A.; Panovska, T. K. Antioxidant and antimicrobial activities of the Pistacia lentiscus and Pistacia atlantica extracts. *Afr. J. Pharm. Pharmacol.* **2008**, *2*, 022–028.

[24]. Al-Snafi, A. E. Constituents and pharmacology of Fumaria officinalis-A review. *J. Pharm.* **2020**, *10* (1), 17–25. http://iosrphr.org/papers/vol10-issue1/C1001011725.pdf (accessed January 20, 2022).

[25]. Turan, S. Ülkemizde Yaygın Olarak Kullanılan Bazı Tıbbi Bitkilerin Yapraklarında Ağır Metal Ve Mineral Besin Element İçeriklerinin Tayini, Ms Dissertation, Marmara Üniversitesi, İstanbul, Türkiye, 2014.

[26]. Dulger, B.; Gonuz, A. Antimicrobial activity of certain plants used in Turkish traditional medicine. *Asian J. Plant Sci.* **2003**, *3*, 104–107.

[27]. Peršin, Z.; Ravber, M.; Stana Kleinschek, K.; Knez, Ž.; Škerget, M.; Kurečič, M. Bio-nanofibrous mats as potential delivering systems of natural substances. *Text. Res. J.* **2017**, *87*, 444–459.

[28]. Doğan, G.; Başal, G.; Bayraktar, O.; Özyildiz, F.; Uzel, A.; Erdoğan, İ. Bioactive Sheath/Core nanofibers containing olive leaf extract: nanofibers containing olive leaf extract. *Microsc. Res. Tech.* **2016**, *79*, 38–49.

[29]. Luque de Castro, M. D.; Priego-Capote, F. Soxhlet extraction: Past and present panacea. *J. Chromatogr. A* **2010**, *1217*, 2383–2389.

[30]. Erdogan, I.; Demir, M.; Bayraktar, O. Olive leaf extract as a crosslinking agent for the preparation of electrospun zein fibers. *J. Appl. Polym. Sci.* **2015**, *132*, 41338.

[31]. Erdogrul, Ö. T. Antibacterial activities of some plant extracts used in folk medicine. *Pharm. Biol.* **2002**, *40*, 269–273.

[32]. Demirpek U. Antimicrobial Susceptibility Tests, Turkish Society of Clinical Microbiology and Infectious Diseases, 2012.

[33]. Huang, Z.-M.; Zhang, Y.-Z.; Kotaki, M.; Ramakrishna, S. A review on polymer nanofibers by electrospinning and their applications in nanocomposites. *Compos. Sci. Technol.* **2003**, *63*, 2223–2253.

[34]. Islam, M. T.; Laing, R. M.; Wilson, C. A.; McConnell, M.; Ali, M. A. Fabrication and characterization of 3-dimensional electrospun poly(vinyl alcohol)/keratin/chitosan nanofibrous scaffold. *Carbohydr. Polym.* **2022**, *275*, 118682.

[35]. Zheng, J.; He, A.; Li, J.; Xu, J.; Han, C. C. Studies on the controlled morphology and wettability of polystyrene surfaces by electrospinning or electrospraying. *Polymer (Guildf.)* **2006**, *47*, 7095–7102.

[36]. Tan, S.-H.; Inai, R.; Kotaki, M.; Ramakrishna, S. Systematic parameter study for ultra-fine fiber fabrication via electrospinning process. *Polymer (Guildf.)* **2005**, *46*, 6128–6134.

[37]. Erdem, R. Nanolif Bazlı Yara Örtüsü Yüzeyi Geliştirilmesi, Ph. D. Dissertation, Marmara Üniversitesi, İstanbul, Türkiye, 2013.

[38]. Rolandi, M.; Rolandi, R. Self-assembled chitin nanofibers and applications. *Adv. Colloid Interface Sci.* **2014**, *207*, 216–222.

[39]. Avci, H.; Gergeroglu, H. Synergistic effects of plant extracts and polymers on structural and antibacterial properties for wound healing. *Polym. Bull. (Berl.)* **2019**, *76*, 3709–3731.

[40]. Kaya, M.; Khadem, S.; Cakmak, Y. S.; Mujtaba, M.; Ilk, S.; Akyuz, L.; Salaberria, A. M.; Labidi, J.; Abdulqadir, A. H.; Deligöz, E. Antioxidative and antimicrobial edible chitosan films blended with stem, leaf and seed extracts of Pistacia terebinthus for active food packaging. *RSC Adv.* **2018**, *8*, 3941–3950.

[41]. Abdullah@Shukry, N. A.; Ahmad Sekak, K.; Ahmad, M. R.; Bustami Effendi, T. J. Characteristics of Electrospun PVA-Aloe vera Nanofibres Produced via Electrospinning. In Proceedings of the International Colloquium in Textile Engineering, Fashion, Apparel and Design 2014 (ICTEFAD 2014); Springer Singapore: Singapore, 2014; pp. 7–11.

[42]. Ikhmal, W. M. K. W. M.; Yasmin, M. Y. N.; Fazira, M. F. M.; Rafizah, W. A. W.; Wan Nik, W. B.; Sabri, M. G. M. Anticorrosion Coating using Olea sp. Leaves Extract. *IOP Conf. Ser. Mater. Sci. Eng.* **2018**, *344*, 012028.

[43]. Bayçin, D.; Altiok, E.; Ulkü, S.; Bayraktar, O. Adsorption of olive leaf (Olea europaea L.) antioxidants on silk fibroin. *J. Agric. Food Chem.* **2007**, *55*, 1227–1236.

[44]. Farah, S.; Anderson, D. G.; Langer, R. Physical and mechanical properties of PLA, and their functions in widespread applications — A comprehensive review. *Adv. Drug Deliv. Rev.* **2016**, *107*, 367–392.

[45]. Yang, S.-L.; Wu, Z.-H.; Yang, W.; Yang, M.-B. Thermal and mechanical properties of chemical crosslinked polylactide (PLA). *Polym. Test.* **2008**, *27*, 957–963.

[46]. Avci, H.; Monticello, R.; Kotek, R. Preparation of antibacterial PVA and PEO nanofibers containing Lawsonia Inermis (henna) leaf extracts. *J. Biomater. Sci. Polym. Ed.* **2013**, *24*, 1815–1830.